

# Contents

<b>6</b>	<b>Discussion</b>	<b>1</b>
6.1	Preventing coarse model instability . . . . .	1
6.2	Strategies for improving subgrid tendency prediction . . . . .	1
6.3	Physical explanation of subgrid tendency correlations . . . . .	2
6.4	Unanswered questions . . . . .	4
6.5	Conclusion . . . . .	4

*This page intentionally left blank*

God does not care about our mathematical difficulties; He integrates empirically.

---

Albert Einstein, quoted by Leopold Infeld in  
*Quest: an autobiography*, 1941

## Chapter 6

# Discussion

TODO: introductory paragraph

### 6.1 Preventing coarse model instability

One of the earliest issues encountered in this work was the potential for low-resolution models to become numerically unstable, making it difficult to obtain a baseline for evaluating parametrised models. Aside from the need for a baseline, it seems unlikely that a simple parametrisation scheme like the one developed in [Chapter 4](#) would have improved the skill of a coarse model on the brink of instability. Since this work was not concerned with accurately representing physical reality, I chose to artificially add hyperviscosity terms to the equations. Another option for future work could be to use stress-free boundary conditions on the top and bottom plates (i.e.,  $w(z = 0, 1) = \partial u / \partial z|_{z=0,1} = 0$ ) rather than the no-slip condition. This could reduce the large near-wall temperature and velocity gradients that often triggered instability at low resolutions.

However, when modelling real-world systems such as the atmosphere, one does not have the freedom to simply alter the governing equations. Successful data-driven parametrisation in these cases will depend on the careful choice of the numerical methods used to discretise and solve the equations such that the underlying coarse model is stable, even if it is inaccurate. Further work with the Rayleigh-Bénard system should investigate whether other types of solvers (finite difference/volume/element, etc.) are more suitable.

### 6.2 Strategies for improving subgrid tendency prediction

Another obstacle to data-driven parametrisation for spatially continuous problems is that there is a very large number of possible subgrid tendency predictors. For Rayleigh-Bénard, one not only has the three prognostic variables, but also their derivatives to arbitrary order in the two spatial directions. The position-dependence of the subgrid tendency statistics was a further complication, adding  $z$  to the list of predictors. One could even use spatially or temporally nonlocal predictors (i.e., the values of the variables at nearby points in space or previous time steps)—a possibility that was not even considered in this work. It would be impossible for a human to explore every possible combination. Supervised machine learning algorithms, discussed briefly in § 1.3.2, are much better-suited to regression problems with large numbers of predictors and could potentially capture hidden and/or nonlinear relationships between these predictors and the subgrid tendencies. There is no doubt, however, that this work was limited by the simplicity of the predictors and regression models that were considered, and future work using more sophisticated statistical models may indeed have greater success without needing to resort to

machine learning.

This work was further limited by its use of purely deterministic parametrisation schemes despite the existence of considerable residuals in the subgrid tendency regressions [Figures 4.8–4.10](#). Stochastic parametrisation, discussed in [§ 1.3.1](#), has the potential to reduce mean-state model biases by emulating the observed residuals. With the tools I have developed for the Rayleigh-Bénard problem, it would be relatively straightforward to experiment with various stochastic perturbations of the existing deterministic scheme (4.4), beginning with those that have been tested for Lorenz '96 (see [§ 2.2](#)). This would include the use of time-correlated (e.g., AR(1)) noise to reflect the persistence (memory) of the subgrid tendencies.

## 6.3 Physical explanation of subgrid tendency correlations

Despite the difficulties described in [§ 6.2](#), the joint histograms in [Chapter 4](#) gave clear evidence of subgrid tendency predictability in the near-wall regions. In this section, I argue that (at least) the correlations involving the  $\theta$  subgrid tendency can be physically explained and are not spurious. As a reminder, the results in question are:

1. The negative correlation between the  $\theta$  subgrid tendency and  $w$  near  $z = 0, 1$ ,
2. The positive correlation between the  $\theta$  subgrid tendency and  $\partial u / \partial x$  near  $z = 0$  and the negative correlation near  $z = 1$ , and
3. The negative correlation between the  $\theta$  subgrid tendency and the  $\theta$  tendency predicted by the coarse model, near  $z = 0, 1$ .

I attribute these to the coarse-graining step, which, in the process of smoothing the temperature field, widens the thermal boundary layer considerably (compare [Figure 4.2a](#) to [Figure 4.2c](#)). On the one hand, there is little change in boundary layer thickness between the coarse state at time  $t$  and the true coarse state at time  $t + \delta t$  because the latter is obtained by first applying the fine model to the fine state at time  $t$  ([Step 1](#)) and then coarse-graining ([Step 2](#)). This means that the true coarse tendencies ([Step 4](#)) are close to zero in the boundary layers. On the other hand, the coarse model prediction for time  $t + \Delta t$  is obtained by first coarse-graining the fine state at time  $t$  ([Step 2](#)) and *then* applying the coarse model ([Step 3](#)). At the high Rayleigh number used here ( $Ra = 10^9$ ), advection in the coarse model immediately begins to thin out the unusually thick boundary layers.

[Figure 6.1](#) gives a cartoon illustration of the effect of advection on the temperature field. Consider the bottom left green dot, which is located near the lower wall, at the base of a rising convection plume. At this point, the vertical velocity  $w$  is positive, and fluid is rushing inwards from the left and right, making  $\partial u / \partial x$  negative. The aforementioned widening of the thermal boundary layer by the coarse-graining operation has effectively created a large mass of warmer fluid beneath; this is advected upwards in the coarse model, meaning that the coarse model predicts a positive tendency  $\partial \theta / \partial t$  at the green dot. As explained in the previous paragraph, the true value of  $\partial \theta / \partial t$  is closer to zero at this point. The subgrid tendency—the true tendency minus predicted tendency—is therefore negative.

Applying the same logic to the other three green dots in [Figure 6.1](#), as shown by the text boxes, one finds that the signs of  $w$  and the predicted tendency are always opposite to the sign of the subgrid tendency. The conclusion is that these variables must be negatively correlated with the subgrid tendency near  $z = 0, 1$ . On the other hand, the  $\partial u / \partial x$  has the same sign as the subgrid tendency near  $z = 0$  (i.e., positive correlation) and the opposite sign near  $z = 1$  (i.e., negative correlation). These predictions are all consistent with the observations in [Chapter 4](#).

It is fairly easy to attribute the subgrid  $\theta$  tendency correlations to advection in the coarse model because  $\theta$  behaves a tracer that is nearly conserved by the flow. The velocity field, however, also has a boundary layer that is widened by the coarse-graining operation, leading me to conjecture that the subgrid  $u$  and

$w$  tendency correlations can be explained using a similar argument. The fact that all the correlations exhibit similar height dependence lends credence to the conjecture. If this is true, then the fact that  $\theta$  is more closely conserved by the flow than  $u$  or  $w$  could explain why the correlations for  $\theta$  were observed to be consistently stronger than the other variables (see, e.g., [Table 4.2](#)).

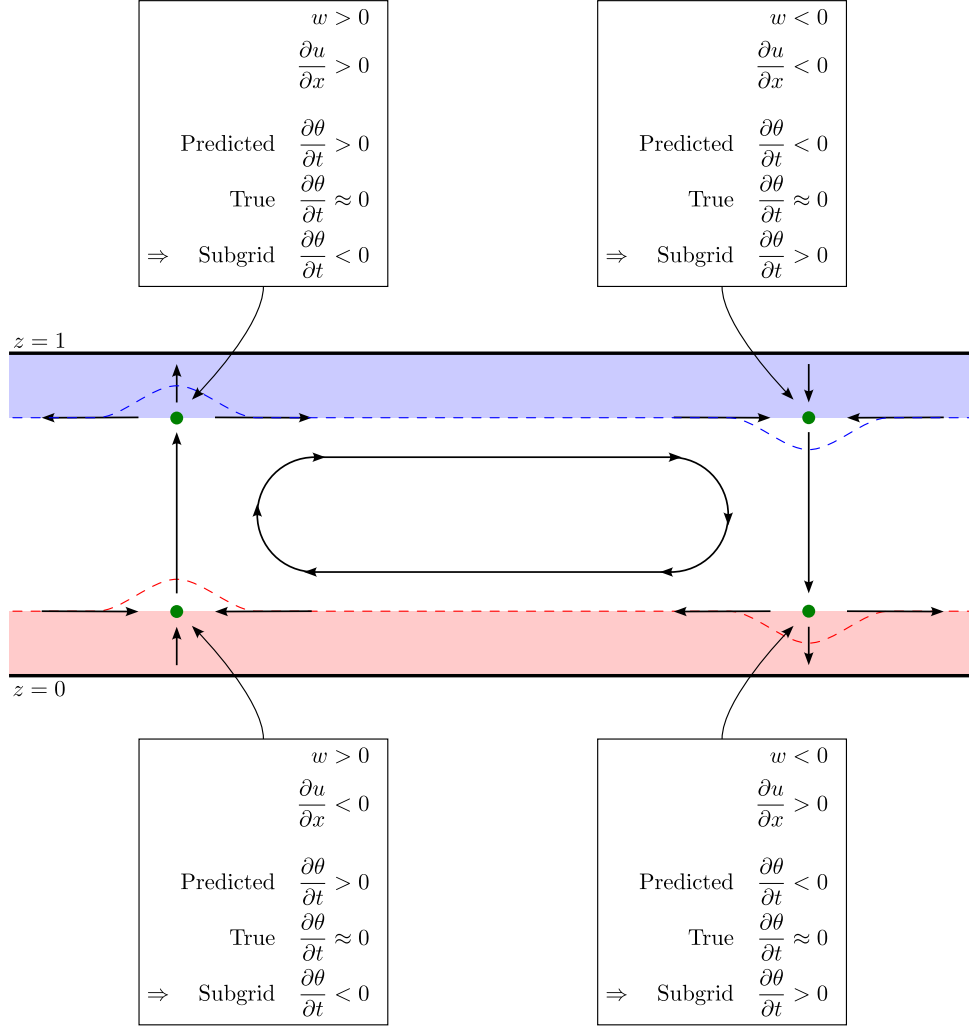


Figure 6.1: Cartoon illustration of the effect of advection on the coarse-grained temperature field when it is evolved using the coarse model. Thick horizontal black lines represent the top and bottom domain walls. Black arrows represent the velocity field. The warm and cold thermal boundary layers are indicated by red and blue shading respectively. Advection deforms the isotherms in the boundary layer, which are initially approximately flat, in the manner indicated by the dashed red and blue lines. The text boxes list the signs of the predictors and predictands at the four green dots, demonstrating the claimed correlations.

While it is not surprising that the subgrid tendency statistics are height-dependent, it is interesting that this work was unable to produce evidence of predictability in the interior of the domain, away from  $z = 0, 1$ . Future work should investigate whether more advanced statistical models and/or machine learning are able to reveal correlations in this region.

## 6.4 Unanswered questions

The amount of effort this work has devoted to overcoming prerequisite issues has inevitably limited the scope of its experimentation with actual parametrisation development and assessment. The positive outcome, however, is that it has implemented the computational tools needed to undertake further research with the Rayleigh-Bénard system and made them publicly available for others to use **TODO: computation section**. There are several worthwhile research questions that could be addressed using these tools.

The foremost goal for future work is to determine the extent to which the inclusion of stochasticity and/or memory in parametrisation schemes can improve their online performance, as well as the optimal method of inclusion. As discussed in [Chapter 1](#), these are topics of considerable research interest in the context of weather and climate modelling. It would be possible to include random forcings in a parametrisation either additively or multiplicatively, and one could also compare the effects of spatially and/or temporally correlated noise to white noise. Online performance could be assessed using the same methods as this work: forecast accuracy using the RMSE of the prognostic variables and time series of domain-averaged metrics, and long-term statistical accuracy using time averages of the same metrics. It would be insightful to also test offline performance more thoroughly, perhaps using the Hellinger distance to measure the agreement between the distributions of predicted and true tendencies (see [§ 2.3.1](#)).

A second important goal is to determine each scheme’s ability to generalise to conditions unseen in its training dataset, such as initial conditions with different numbers of convection cells or changes in Rayleigh number or domain aspect ratio. The findings could inform the development of parametrisations for climate models whose effectiveness is robust in warming conditions—an important goal of modern research.

With a wider variety of statistical models for the subgrid tendencies in combination with a range of stochastic perturbation schemes (with different noise amplitudes, correlation times, etc.), it would be possible to determine whether schemes that perform well offline generally also perform well online, and whether or not their short-term forecast accuracy is correlated with their long-term statistical accuracy. These have been topics of for the Lorenz ’96 system (see [§ 2.5](#)), and an extension to Rayleigh-Bénard could provide further evidence to aid the selection of parametrisation schemes for weather and climate models.

## 6.5 Conclusion

Motivated by previous studies on the Lorenz ’96 system and open questions in weather and climate modelling that call for experimentation in more realistic test frameworks, I have implemented a complete proof of concept for data-driven parametrisation in Rayleigh-Bénard convection. Given a high-resolution “truth” model of the flow and a low-resolution baseline model, straightforward mathematical arguments in [Chapter 1](#) justified a method for calculating the subgrid tendency of each prognostic variable—that is, the contribution of small-scale processes unresolvable by the coarse model to the rate of change of the large-scale state that it could resolve. The method was implemented in [Chapter 4](#) and involved systematic coarse-graining of a high-resolution training simulation and time-stepping with the low-resolution model.

Exploratory analysis in [§ 4.3](#) revealed several correlations between the subgrid tendencies and the large-scale state of the coarse model. The correlations were all strongly conditional on vertical position, appearing to exist only near the top and bottom boundaries of the domain. The most notable of these was a negative linear correlation between the subgrid tendency of each variable and the corresponding tendency predicted by the low-resolution model. A simple parametrisation scheme for predicting the subgrid tendencies based on this relationship was fitted to the training dataset and coupled into the low-resolution model to emulate the effect of the unresolved processes.

Running online, the parametrisation scheme was found to improve the forecast accuracy of the coarse model, but only for short lead times. It was also found to improve long-term statistical accuracy, reducing

the relative error of some metrics by as much as one half. This work therefore provides, from first principles, evidence that data-driven parametrisation is a viable method for improving the skill of low-resolution weather and climate models.

The process of parametrisation development for the Rayleigh-Bénard problem highlighted subtle technical obstacles that do not apply to simpler systems such as Lorenz '96. Firstly, coarse models were prone to numerical instability, necessitating a hyperdiffusive modification of the governing equations. Secondly, the predictability of the subgrid tendencies was found to depend strongly on the method used to coarse-grain the high-resolution solutions, and the development of an appropriate method was non-trivial. The understanding of these issues and the development of computational tools to address them is a second major outcome of this work.

Future work will be able to use and extend the tools established here to perform further parametrisation experiments, addressing important unanswered questions that relate to parametrisation in real weather and climate models. Although it remains an idealised system, Rayleigh-Bénard convection has proven to be a highly instructive test problem and there are no doubt many more lessons to be learnt from it in the future.